Hindawi
Advances in Materials Science and Engineering
Volume 2023, Article ID 9002743, 12 pages
https://doi.org/10.1155/2023/9002743

Research Article

An Optimisation Method of Construction for Warping Copper Plates and Engines Using Complete Block Designs with Some Special Types of Graphs

P. Karthikeyan,[1] K. Kalaiselvi,[1] M. Pachamuthu,[2] Kanulla Karthik,[3] and A. Johnson Santhosh[4]

[1]*Department of Mathematics, Sri Vasavi College of Arts and Science College, Erode, Tamilnadu, India*
[2]*Department of Statistics, Periyar University, Salem, Tamil Nadu, India*
[3]*Department of Mechanical Engineering, Lakireddy Bali Reddy College of Engineering, NTR District, Mylavaram, Krishna, Andhra Pradesh, India*
[4]*Faculty of Mechanical Engineering, Jimma Institute of Technology, Jimma University, Jimma, Ethiopia*

Correspondence should be addressed to A. Johnson Santhosh; johnson.antony@ju.edu.et

Received 15 July 2022; Revised 1 October 2022; Accepted 3 October 2022; Published 31 January 2023

Academic Editor: Vijayananth Kavimani

Copyright © 2023 P. Karthikeyan et al. This is an open access article distributed under the Creative Commons Attribution License, which permits unrestricted use, distribution, and reproduction in any medium, provided the original work is properly cited.

The application of bipartite and regular graphs plays a vital role in the area of engineering, mathematical sciences, design of experiments, and medical fields. This study proposes an optimization method for constriction of randomized block design and Latin square design using bipartite and regular graphs with applications of warping copper plates in specimens and comparing them to burners and engines on different days. The construction methods and analysis are performed as follows: the first method is a construction of randomized block design using bipartite and complete bipartite graphs with applications for the amount of warping copper plates and different laboratories are taken to test any significant difference that exists between the mean number of responses for the labs and copper specimens. The second method is the construction of a Latin square design using regular graphs to test whether there is any significant difference between the burners, engines, and some days in statistical analysis of interaction plots, contour plots, and 3D surface plots.

1. Introduction

In this modern scientific electronic world, mathematical sciences and engineering for a method of construction in complete block designs are randomized block design (RBD) and latin square design (LSD) which have been developed by graph theory. To meet the current trend of warping copper plates and specimens, compared to burners, engines with the statistical analysis problem have become a critical issue, which occurs from the residual stress accumulated from various methods of construction. In this situation inevitable for a method of construction using graph theory incomplete block designs. The first study in graph theory was written by Euler in 1936 when he settled the famous unsolved problem of his day, known as the Konigsberg bridge problem. The graphs over a framework answer issues with several preparations, networking, optimization, matching, and operational problems. For illustration, Google maps use graphs for structure alteration systems, where the connexion of two or more roads is measured to be a vertex, and the road joining two vertices is deemed to be an edge, thus their steering system is based on the procedure to calculate the shortest path between two vertices. In graph theory, as described by Bondy and Murty [1], a component that allows exhibiting a series of data on a chart is known as a bar graph. Any binary vertices combined by more than one edge are known as a multigraph. A graph without loops and with at most one edge between two vertices is called a simple graph. Each vertex is associated by an edge to each other vertex is called a complete graph. Direction may be allocated to each edge to produce is known as a directed graph. A tree suggests splitting out from a root and never implementing a cycle. The applications of trees in data storage, searching, complete block designs, etc. A graph with no cycle is acyclic, a forest is an acyclic graph. A tree is connected acyclic graph. A leaf or pendant vertex is a vertex of degree. A spanning subgraph G is a subgraph with vertex set V (G). A spanning tree is a spanning subgraph that is a tree. For example, a tree is a connected forest, and every component of a forest is a tree. A graph with no cycles has no odd cycles; hence trees and forests are bipartite. The path is a tree, and a tree is a path if and only if its maximum degree is 2. A star is a tree consisting of one vertex adjacent to all the others. The n-vertex star is a biclique $K_{1,n-1}$. A graph that is a tree that has exactly one spanning tree; the full graph itself. In an experimental design, by Das and Giri, [2], the designs containing the basic principle of blocking are called block designs and may be categorized into two types, complete and incomplete block designs. In a complete block design, all the treatments are allocated to every block. That is $k = v$ and hence $b = r$ otherwise incomplete block designs. The experimental material is to be homogeneous, then the design is known as a completely randomized design (CRD). In a CRD, there is no local control measure adopted, and the total variation is divided into two components, treatment and error. An improvement of CRD is obtained by providing local control measures through a blocking design called RBD. Blocking basic principles can be extended more to advance RBD by eliminating more sources of variation. LSD is an improved design with binary sources of variation in two directions, namely, blocks and treatments. Some methods for construction and analysis developed by various researchers concerning such designs are discussed; Bose [3], has discussed the construction of balanced incomplete block designs with an example. Yamamoto et al.[4] has discussed the claw decomposition of complete graphs and complete bipartite graphs. Zhang and Zhu [5] have discussed Hilton's theorem and proved that graph G is a 2-connected, k-regular, nonbipartite graph of order at most $3k - 3$, and x, y is a pair of distinct vertices. If G $\{x, y\}$ is connected, then G contains an (x, y)-Hamilton path. Zhang et al. [6] have developed the effect of underfilled epoxy on warpage in flip-chip assemblies. Jacobs et al. [7] constructed protein flexibility predictions using graph theory. Gavrilyuk and Makhnev [8] have discussed the amply regular graphs and block designs. Tseng et al. [9] have discussed the analysis of the formability of aluminum and copper-clad metals with different thicknesses by the finite element method and experiment. Rizzo and Mansano [10] have developed the electrooptically sensitive diamond-like carbon thin films deposited by reactive magnetron sputtering for electronic device applications. Miyajima et al. [11] have presented the electrophoretic deposition onto an insulator for thin film preparation for electronic device fabrication. Yang et al. [12] have developed the chip warpage model for reliable prediction of delamination failures. Pachamuthu M and Jaisankar R [13] have discussed the construction methodology of lattice designs using *MOLS* using Galois field. Gupta et al. [14] have proved the reduction of out-of-plane warpage in surface micromachined beams using corrugation. Federer and Wright [15] have constructed the lattice square designs. Hwang and Tzou [16] have studied an analytical approach to asymmetrical cold- and hot-rolling of clad sheets using the slab method. Lee et al. [17], analyzed the differential speed rolling to reduce warping in the bimetallic slab. Zhu et al. [18] have discussed the experimental identification of warpage origination during the wafer-level packaging process. Kim et al. [19] have discussed the warpage analysis of electroplated Cu films on fibers-reinforced polymer packaging substrates. The analysis method is performed using the following sequence: fabricate specimens for scanning 3D contours, transform 3D data into curvatures, compute the built-in stress of the film using a stress-curvature analytic model, and verify it through comparisons of the finite element method (FEM) simulations with the measured data also calculate residual stress, and predict curvatures using FEM simulation throughout the reflow process temperature ranging between 25 and 180°C are proven to be accurate by the comparison of the FEM simulations and experimental measurements. Lee [20] have developed the decomposition of the complete bipartite multigraph into cycles and stars. Mandal and Dash [21] have discussed the balanced incomplete Latin square designs with proposed three methods of construction of balanced incomplete latin square designs. Particular classes of Latin squares, namely, Knut Vik designs, semi-Knut Vik designs, and crisscross Latin squares play a key role in the construction. Sumaiya et al. [22] have constructed a generation of complete bipartite graphs using normalized Hadamard matrices. Ramya and Pachamuthu [23] have constructed the balanced incomplete block designs through factorization and coloring graphs using mutually orthogonal Latin square designs with numerical examples. Ilayaraja and Muthusamy [24] have discussed the essential and adequate conditions for the existence of a decomposition of complete bipartite graphs into cycles and stars with four edges of the problems. Sivamaran et al. [25] have studied the effect of chemical vapor deposition parameters on the diameter of multiwalled carbon nanotubes. Sivamaran et al. [26] have discussed optimizing chemical vapor deposition parameters to attain minimum diameter carbon nanotubes by response surface methodology. Nemitallah et al. [27] have reviewed frontiers in combustion techniques and burner designs for emissions control and CO_2 capture. Sivamaran et al. [28] have identified of appropriate catalyst system for the growth of multiwalled carbon nanotubes via a catalytic chemical vapor deposition process in a single-step batch technique. Reddy and Hemavathi [29] have described several characterizations of k-distance bipartite graphs with an example. Saurabh and Singh [30] have discussed a note on the construction of Latin square-type designs. Ozkan [31] has performed a comparative study on the investigation of the electromagnetic shielding performance of copper plate and copper composite fabrics. Electromagnetic shielding performances of copper plate and metal composite in woven/knitted fabrics were compared. For this purpose, the electromagnetic shielding effectiveness of single and double-layer copper plates and metal composite fabrics were measured in vertical and horizontal directions. As a result, the copper plate showed better performance than composite fabric samples for both measurement directions. In general, the EMSE of the composite fabrics was lower than 10 dB for horizontal directions. Only the copper plates provided electromagnetic shielding at a significant level (up to 60 dB) against horizontally polarized waves. EMSE behavior of copper plate was similar for both directions due to the isotropic structure and this performance was maintained at a higher frequency level. On the other hand, gaps in the structure of composite fabrics caused a decrease in EMSE performance against increasing frequency. Raza and Asif Masood [32] have discussed the efficiency of Lattice design in relation to randomized complete block design in agricultural field experiments. Richthammer [33] has derived the bunkbed conjecture for complete bipartite graphs and related classes of graphs. Braun and Tyagi [34] have proved the minimax optimal clustering of bipartite graphs with a generalized power method. Sivamaran et al. [35] have developed multiresponse optimization on tribo-mechanical properties of CNTs/nSiC reinforced hybrid Al MMC through response surface method approach and also studied the optimum parameters were found load at 2.00 kg, speed 200 rpm, 7.50% of SiC reinforcement results in wear rate of 20.50 μm/g with the hardness of 161.43 HV. Moreover, the L32 orthogonal array and hierarchical clustering were established to understand and validate the relationship between the process parameters and responses of this investigation. In this study, an optimization method for the construction of complete block designs is RBD and LSD. The method of construction for RBD and LSD with numerical examples is to test whether there is any significant difference between labs and warping copper plates with specimens, compare three burners, engines and three days is discussed, construing the graphs of results is an interaction plot for response lines around parallel, the R^2 value is nearest to 1, the noise signal is greater than 4, the variables are associated with changes in the response variable, and the contour plot the association between the variables excellence. Also, the graph of three-dimensional (3D) surface plot is related to the response variable, so our hypothesis of the study is valid and significant.

2. Preliminaries

2.1. A Bipartite Graph. A graph $G = (V, E)$ is said to be a bipartite graph if vertices set V can be separated into two subsets V_1 and V_2, such that each edge of G connects a vertex of V_1 to V_2. These graphs are meant by $K_{m,\,n}$, where m and n are the numbers of vertices in V_1 and V_2, respectively.

2.2. A Complete Bipartite Graph. A graph $G = (V, E)$ is a complete bipartite graph if vertices set V can be separated into two subsets V_1 and V_2, so each vertex of V_1 is connected to each vertex of V_2. The number of edges in a complete bipartite graph is $m \times n$ as each of the m vertices is connected to each of the n vertices.

2.3. Randomized Block Design (RBD). The RBD of each treatment is repeated the same number of times. Suppose that there are v treatments, and each v is to be repeated r times and the total number of the experimental units is vr; then, these are arranged into b groups, each of size k, and these groups are made homogeneous using the error control measure, and then the v treatments are allotted at random to the k plots in each block. This type of homogeneous grouping of the experimental units and the random allocation are the features of RBD.

2.4. Latin Square Design (LSD). A Latin square is designed to arrange $(n \times n)$ different treatments so that each treatment occurs exactly once in each row and each column.

2.5. Regular Graph. The degree of a vertex v in graph G written as $d_g\,(v)$ is the number of edges incident to v, except

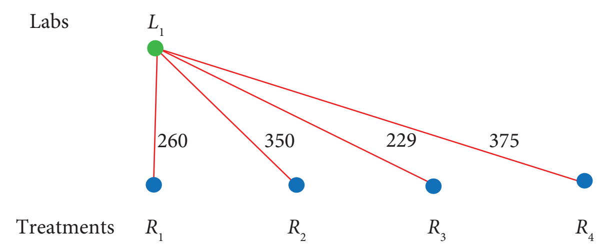

Figure 1: First bipartite graph.

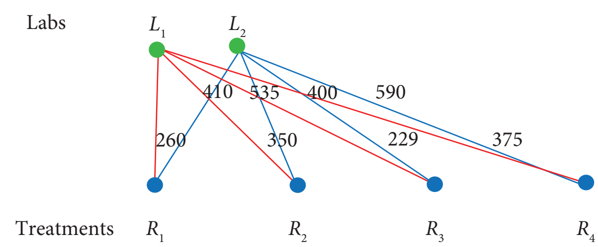

Figure 2: Second bipartite graph.

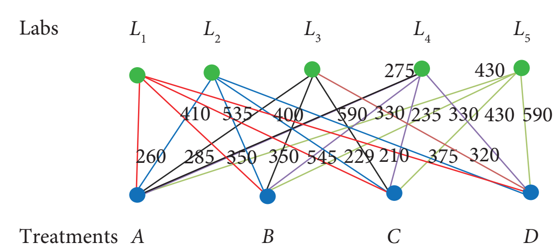

Figure 3: Third bipartite graph.

Table 1: Labs and warping copper plates and specimens.

Labs	Warping copper plates and specimens (treatments)			
	A	B	C	D
L_1	260	350	229	375
L_2	410	535	400	590
L_3	285	350	210	320
L_4	275	330	235	330
L_5	430	545	430	590

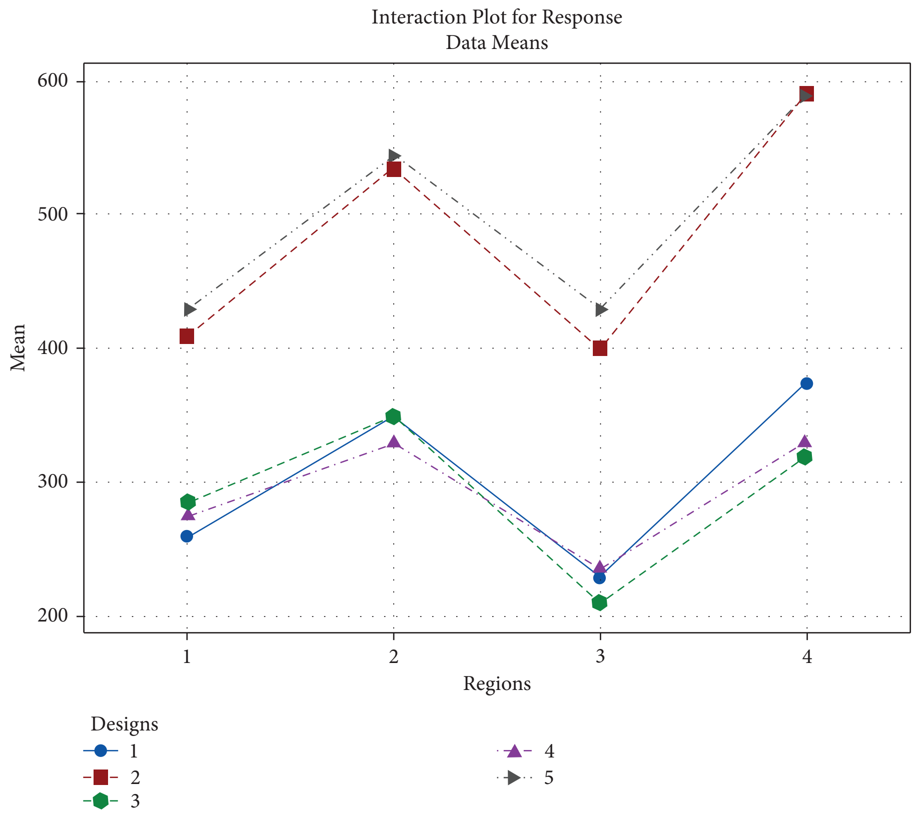

Figure 4: Interaction plot for response.

Table 2: Model summary.

S	R^2 (%)	Adj. R^2 (%)	Predicted R^2 (%)
27.0372	96.66	94.71	90.72

Table 3: Coefficients of response.

Term	Coeff	SE. Coeff	T-value	P value	VIF
Constant	373.95	6.05	61.85	0.01	
Labs					
1	−70.5	12.1	−5.83	0.01	1.60
2	109.8	12.1	9.08	0.01	1.60
3	−82.7	12.1	−6.84	0.01	1.60
4	−81.4	12.1	−6.74	0.01	1.60
Treatments					
1	−42.0	10.5	−4.01	0.02	1.50
2	48.0	10.5	4.59	0.01	1.50
3	−73.1	10.5	−6.99	0.01	1.50

that each loop at v is counted twice. The maximum degree is $\triangle(G)$, the minimum degree is $\delta(G)$, and G is regular if $\triangle(G) = \delta(G)$.

3. Main Results

3.1. An Optimisation of Techniques for Warping Copper Plates and Specimens Method of Construction for RBD Using Bipartite and Complete Bipartite Graphs

Step 1: Let us consider any RBD order layout $(b \times v)$ and take rows considered blocks (b) and columns considered treatments (v). Complete the vertices of the graph set V and separate the vertices set into two subsets V_1 and V_2.

Step 2: connect every vertex in V_1toV_2 by using the edges for both the bipartite and complete bipartite graphs

Step 3: if the number of v is equal to the number of blocks $(b = v)$, then the complete bipartite graph is used instead of a portion of the bipartite graph

Step 4: all edges in a complete bipartite graph is $(b \times v)$

Step 5: thus, the same procedure is used to draw a graph for all the different orders $(b \times v)$ of *RBD*

3.2. Applications

3.2.1. Example 1. An experiment to determine the amount of warping (mm) of copper plates was conducted in five different laboratories (L_1, L_2, L_3, L_4, and L_5) using four copper specimens (treatments) with different percentage of copper compositions (A, B, C, and D).

Step 1: Construction of the above experiment is to form an RBD layout of five laboratories and four copper specimens . Consider the first lab (L1) to be given four treatments (A=R_1, B=R_2, C=R_3, and D=R_4); the amount of warping (mm) of copper plates value is R_1=260,

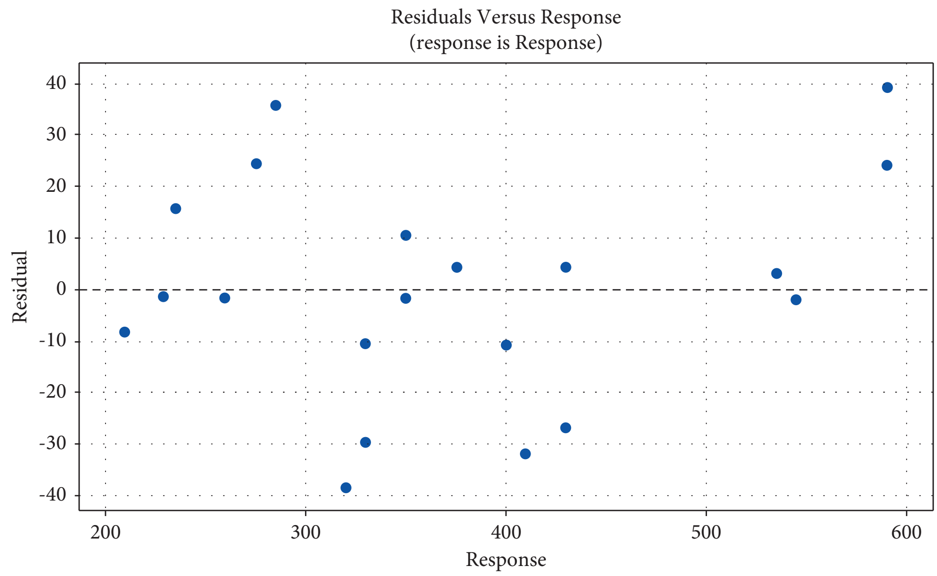

Figure 5: Residuals versus response.

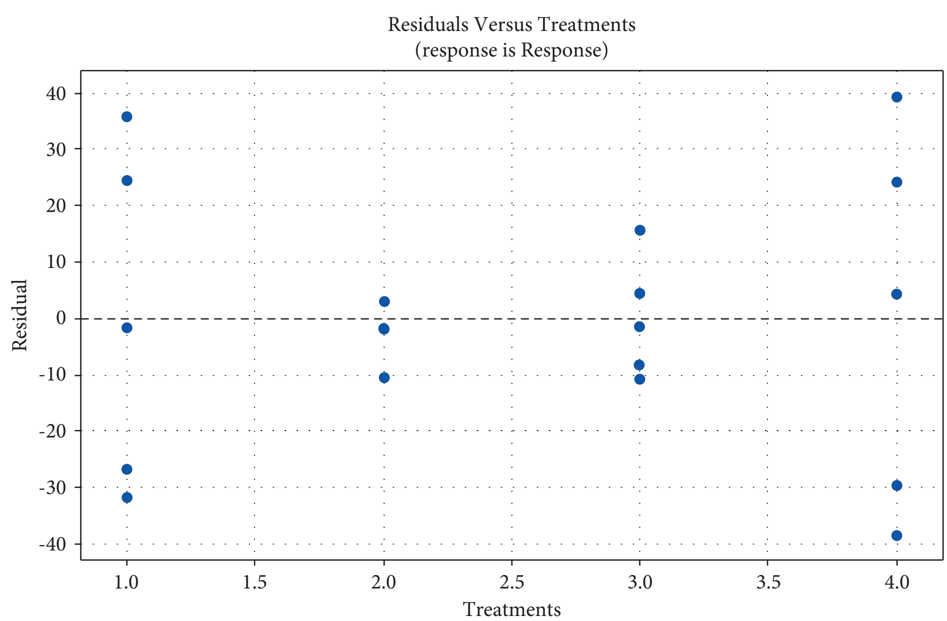

Figure 6: Residuals versus treatments.

$R_2 = 350$, $R_3 = 229$, and $R_4 = 375$, and resulting Figure 1 is known as first bipartite graph as follows:

Step 2: Consider the second lab (L2) given for four treatments (A, B, C, and D) the amount for warping (mm) of copper plates in 410, 535, 400, and 590 respectively. Using complete bipartite graphs and construction of separate the vertices set V into four subsets $A = V_1 = R_1, B = V_2 = R_2, C = V_3 = R_3$ and $D = V_4 = R_4$, the labs and specimens (treatments) are given the second bipartite graph in Figure 2 as follows;

Step 3: Similarly, using the above steps of the same procedure for constructing the third, fourth, and fifth labs (L3, L5, and L5) in four treatments. Observe the data of the third lab value is 285, 350, 210, and 320; the fourth lab value is 275, 330, 235, and 330; the fifth lab value is 430, 545, 430, and 590. Using complete bipartite graphs and constructing to separate the vertices set V into four subsets $A = V_1 = R_1, B = V_2 = R_2, C = V_3 = R_3$ and $D = V_4 = R_4$, the labs and specimens (treatments) given the third bipartite graph in Figure 3 are as follows;

Since there are five labs and four specimens, the amount of warping (mm) of copper plates is shown in Table 1.

Discuss if any significant difference exists between the mean number of responses for the five labs and four copper specimens.

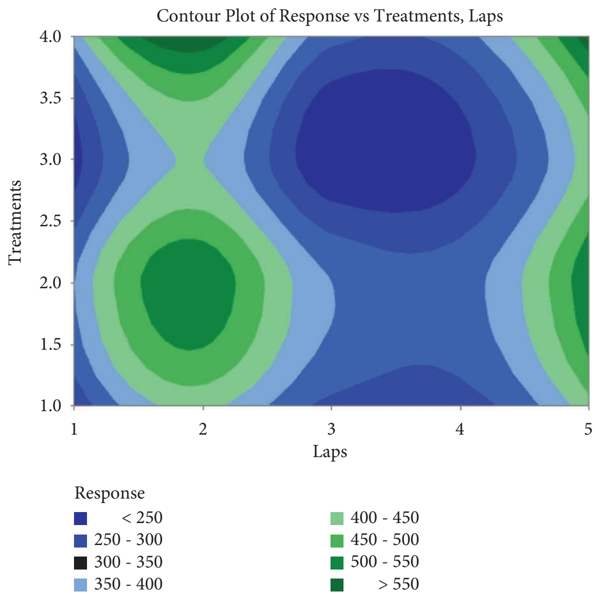

Figure 7: Contour plot of response vs. treatments vs. labs.

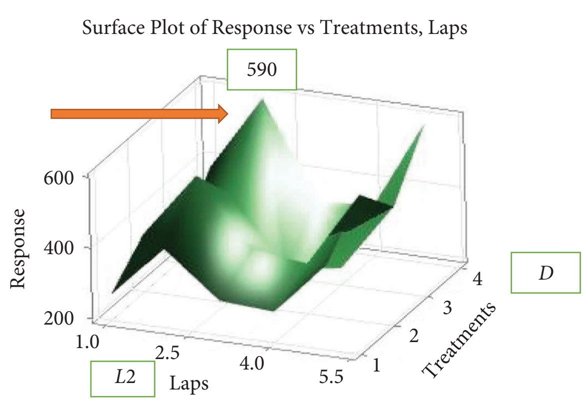

Figure 8: Surface plot of response vs. treatments vs. labs.

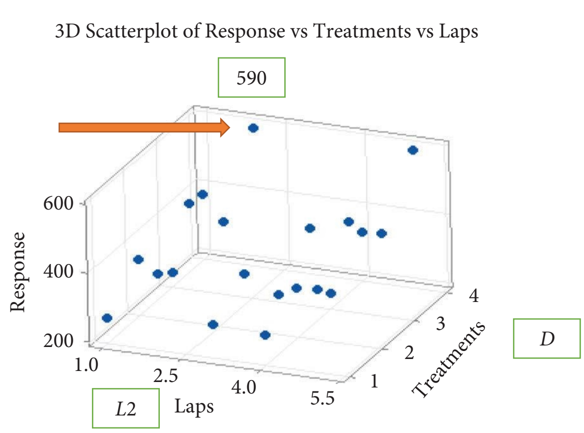

Figure 9: 3D scatterplot of response vs treatments vs labs.

Solution: constructing the graphs. The below interaction plot Figure 4 for response lines around parallel. So, our hypothesis of the study is valid and continues with the analysis.

Table 4: ANOVA for response.

SV	df	Adj. SS	Adj. MS	F-value	P value	Remarks
Labs	4	184271	46067.7	63.02	0.01	Significant
Copper specimens	3	69576	23192.0	31.73	0.01	Significant
Error	12	8772	731.0	—	—	—
Total	19	262619	—	—	—	—

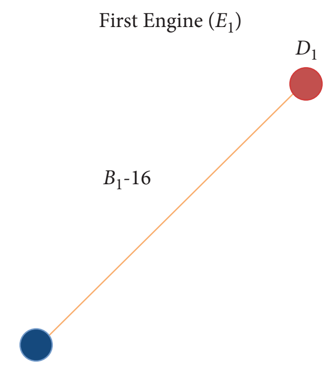

Figure 10: First regular graph.

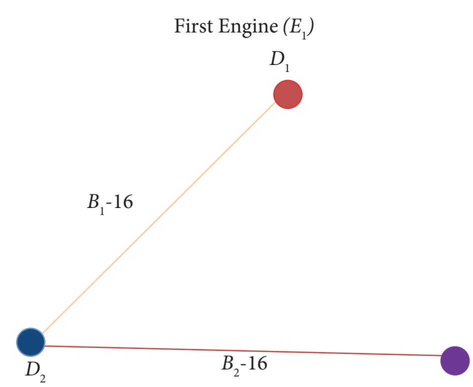

Figure 11: Second regular graph.

Null hypothesis (H_0): there is no significant difference between labs and copper specimens.

In Table 2, the R^2 value is nearest to 1 (0.9666) and the model is fitted to our problem. The R^2 probability value is 0 to 1. The difference is very close R^2 to the adjusted R^2 of 0.9072 and the noise signal is greater than 4 (27). A predicted R^2 value is 90.72% which is substantially less than the R^2 value of 96.66% which may indicate the overall model is fitted in the abovementioned example.

The coefficient response in Table 3 for two factors labs and copper specimens is significant at a 5% level of significance and concludes that the variables are associated with changes in the response variable.

3.2.2. General Linear Model: Response versus Labs and Treatments. In Figures 5 and 6 the normality and equal variance (treatments, residual response) assumptions are responsible. There is no concern, however, about the

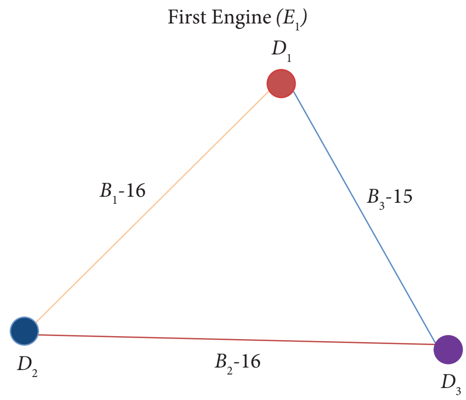

Figure 12: Third regular graph.

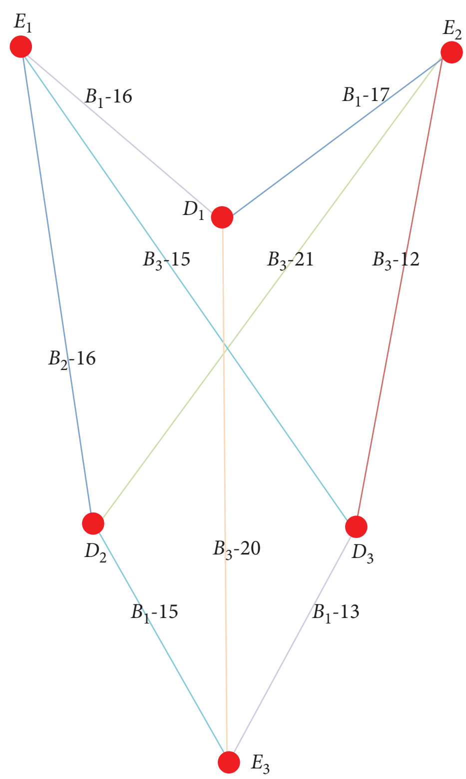

Figure 13: Fourth regular graph.

Table 5: Burners, engines, and days.

-	Engine 1	Engine 2	Engine 3
Day 1	Burner 1-016	Burner 2-017	Burner 3-020
Day 2	Burner 2-016	Burner 3-021	Burner 1-015
Day 3	Burner 3-015	Burner 1-012	Burner 2-013

appropriateness of the no interaction assumption. The data appear to be randomly distributed at the center line zero. Now, we perform an analysis for a randomized block design.

3.2.3. Contour Plot of Response vs. Treatments vs. Labs. The contour plot (Figure 7) indicates two predictor variables and shows the association between the variables labs

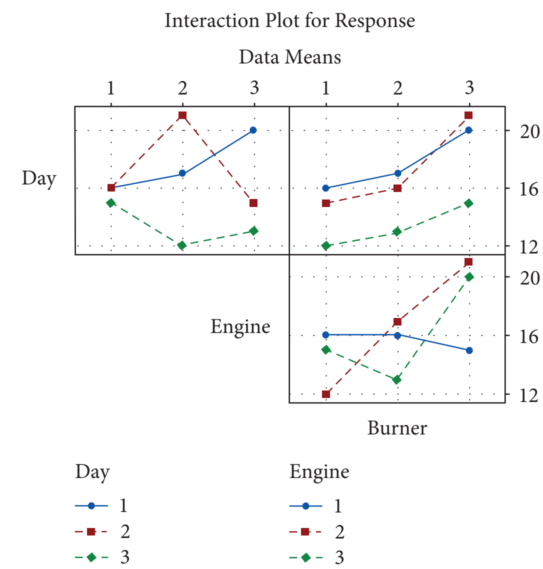

Figure 14: Interaction plot for response.

Table 6: Model summary.

S	R^2 (%)	Adj. R^2 (%)	Predicted R^2 (%)
0.881917	97.74	90.97	54.27

Table 7: Coefficients of response.

Term	Coef	Coef	T-value	P value	VIF
Constant	16.111	0.294	54.80	0.001	1.33
			Days		
1	1.556	0.416	3.74	0.065	1.33
2	1.222	0.416	2.94	0.099	1.33
			Engines		
1	−0.444	0.416	−1.07	0.397	1.33
2	0.556	0.416	1.34	0.313	1.33
			Burners		
1	−1.778	0.416	−4.28	0.051	1.33
2	−0.778	0.416	−1.87	0.202	1.33

(L_2) and treatment (D) used for the amount of warping (mm) of copper plates. The dark areas of the plot specify excellence. Figure 8 indicates three dimensional (3D) and Figure 9 is a surface plot of illustration into two predictor variables and related the response variable is normal as follows.

3.2.4. The 3D Surface Plot of Response vs. Treatments vs. Labs. The conclusion of the plots in Figures 8 and 9 shows that the relationship between the two variables labs and treatments for the amount of warping (mm) of copper plates occurs at nearly the second lab = 590 and treatments = D. All the sum of squares are presented in Table 4 and an inference is drawn.

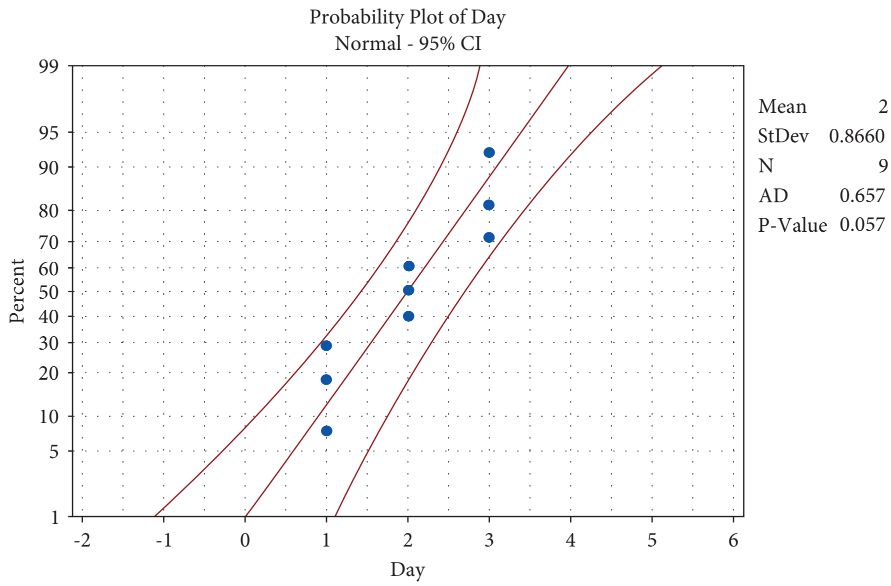

Figure 15: Probability plot of day.

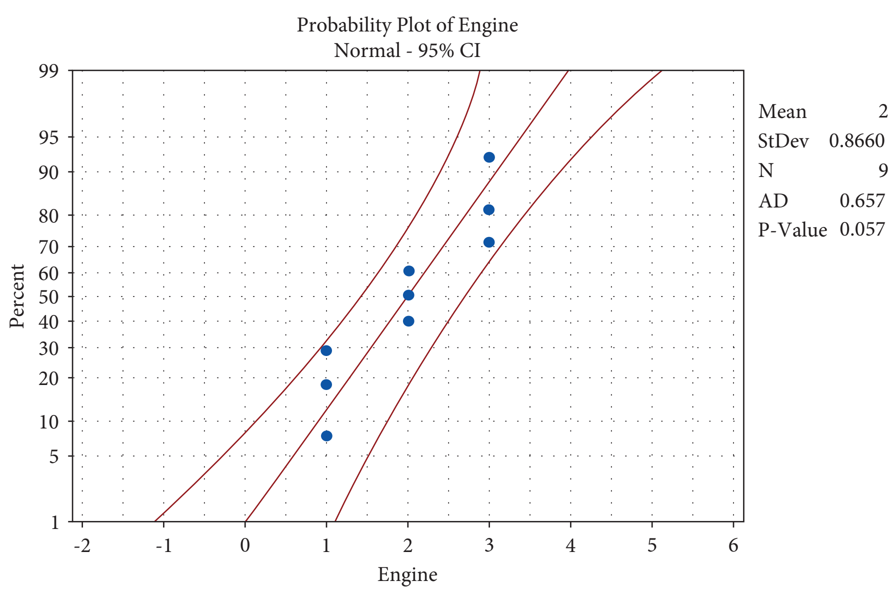

Figure 16: Probability plot of engine.

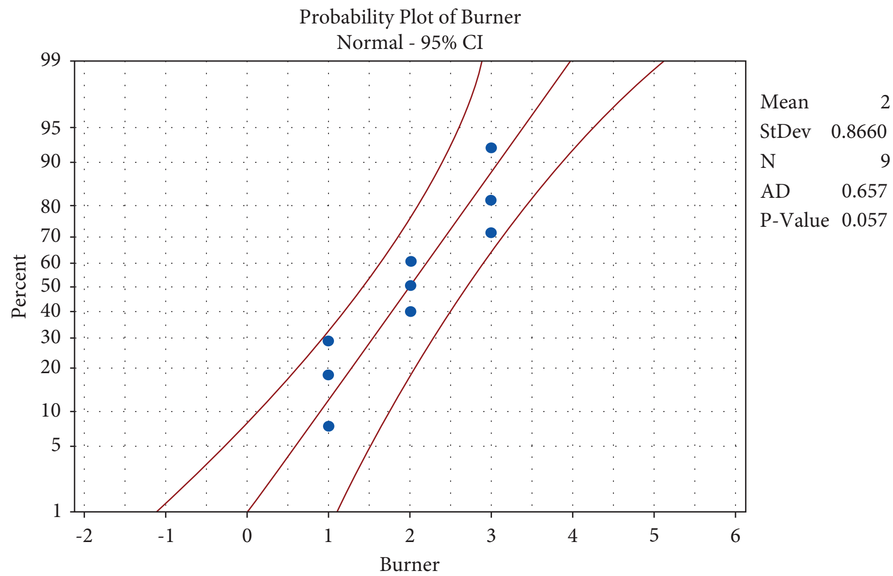

Figure 17: Residuals versus burner.

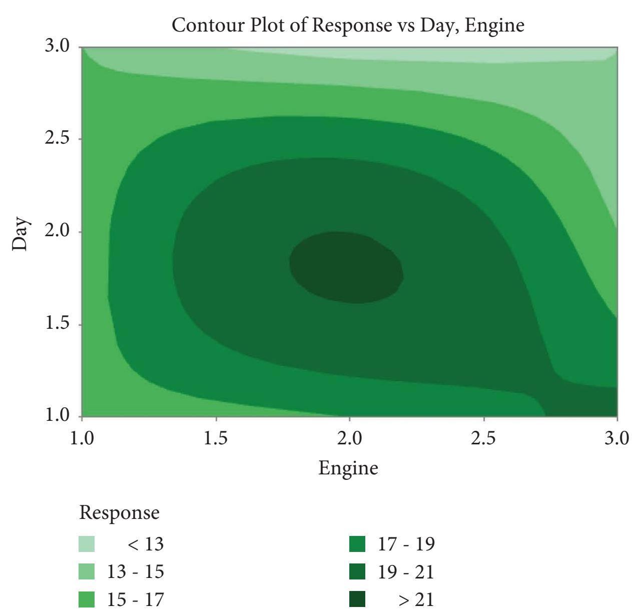

Figure 18: Contour plot of response vs. day vs. engine.

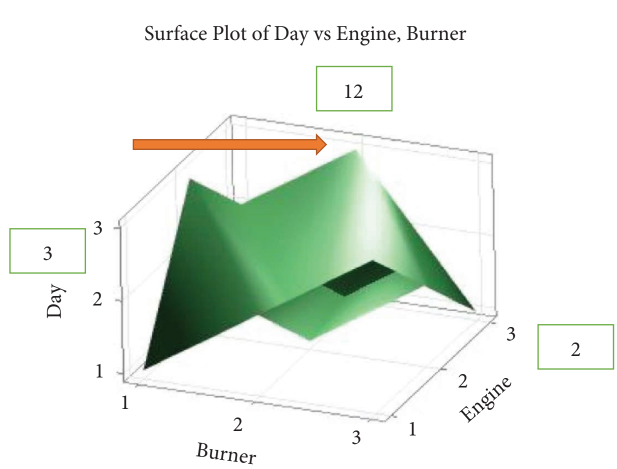

Figure 19: 3D plots of day vs. engine and burner.

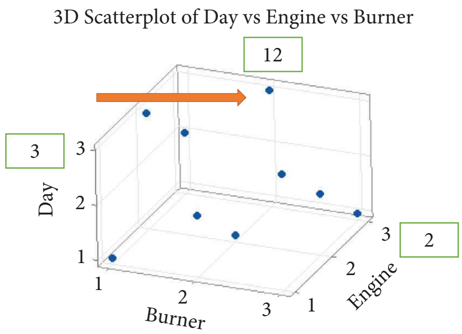

Figure 20: 3-D day vs engine vs. burner.

Table 8: ANOVA for the response.

sv	df	Adj. SS	Adj. MS	F-value	P value	Remarks
Days	2	34.889	17.4444	22.43	0.043	Significant
Engines	2	1.556	0.7778	1.00	0.500	Not significant
Burners	2	30.889	15.4444	19.86	0.048	Significant
Error	2	1.556	0.7778	—	—	—
Total	8	68.889	—	—	—	—

(1) Inference. Since P is 0.0, the model F-value (63.02) suggests that the model is significant. There is only a 0.01% chance that an F-value this large could occur due to noise.

3.3. An Optimisation Method of Construction for Burners and Engines using LSD with Regular Graph

Step 1: Take any LSD of order $(n \times n)$, the rows and treatments are considered as two sets of vertices, and then differentiate both by using vertex coloring.

Step 2: The regular graph has the same degree of vertices. Each vertex is connected to other vertices with the same number of edges.

Step 3: If the treatment numbers are equal to the blocks $(b = v)$, then the complete bipartite graph is used instead of a portion of the bipartite graph, and the edge numbers in the regular graph are $(n \times n)$.

Step 4: Thus, the same procedure is used to draw the graph for all the different orders n of *LSD*.

3.4. Applications

3.4.1. Example 2. A trial to compare three burners B_1, $B_{2,}$ and B_3, three engines E_1, E_2, and $E_{3,,}$ and three days D_1, $D_{2,}$ and D_3 is given as follows:

Step 1: let us consider the first day (D1), first burner (B1), and first engine (E1) and are taken two sets of vertices and differentiate both of them by using vertex coloring of the regular graph to construct these three directions of factors for the results is 16 hours are shown in Figure 10 as follows;

Step 2: Consider the second day (D2), second burner (B2), and second engine (E2) and are taken as two sets of vertices and differentiate both of them by using vertex coloring of the regular graph to the construction of these three directions of factors for the results is 16 hours are shown in Figure 11 as follows;

Step 3: The third day (D3), third burner (B3), and third engine (E3) are taken as two sets of vertices and differentiated of them by using vertex coloring of the regular graph to the construction of these three directions of factors for the results is 15 hours are shown in Figure 12 as follows;

Step 4: Similarly, the same procedure to constriction of the regular graph using the remaining day, burner, and two engines the resulting diagram is known as the regular graph has the same degree of all vertices that is every vertex connected to any other vertices with the same number of edges are shown in Figure 13 as follows;

Step 5: The days are equal to the engines $(b = v)$ and number of burners; then, the complete bipartite graph is used instead of the bipartite graph, and the number of edges in the regular graph is (3×3). A LSD was formed as the tests were made on three engines (E1, E2, and E3) and were spared over three days (D1, D2, and D3). Since there are three burners, three engines, and three days values are shown below in Table 5.

To check whether the null hypothesis is that there is any significant difference between the burners, engines, and number of days.

(1) Solution: constructing the graphs. The plot in Figure 14 is referred to as the interaction of the lines that are not parallel and the interaction result specifies that the association between burners and engines depends on the value of days.

Null hypothesis (H_0): there is no significant difference between burners, days, and engines.

Table 6 represents that the model is fitted because the R^2 value is nearest to 1 (0.9774). The probability R^2 value is 0 to 1. The difference is very close R^2 to the adjusted R^2 of 0.9072 and the noise signal is greater than 4 (88). A predicted R^2 value is 54.27% which is substantially less than the R^2 value of 97.74% which may indicate that the overall model is fitted in the abovementioned example.

The coefficient response in Table 7 for three factors day and burner is significant, but the engine is not significant at a 5% level of significance and concludes that the variables are associated with changes in the response variable.

3.4.2. Probability Plot of Day. In the probability plot of the day (Figure 15), the null hypothesis states that the data follow a normal distribution. The fitted distribution line is the straight middle line on the plot. The outer solid lines on the plot are confidence intervals for the individual percentiles, not for the distribution as a whole, and should not be used to assess distribution fit.

3.4.3. Probability Plot of Engine. In the probability plot of the engine (Figure 16), the null hypothesis states that the data follow a normal distribution. The fitted distribution line is the straight middle line on the plot. The outer solid lines on the plot are confidence intervals for the individual percentiles, not for the distribution as a whole, and should not be used to assess distribution fit.

3.4.4. Probability Plot of Burner. In the probability plot of the burner (Figure 17), the null hypothesis states that the data follow a normal distribution. The fitted distribution line is the straight middle line on the plot. The outer solid lines on the plot are confidence intervals for the individual percentiles, not for the distribution as a whole, and should not be used to assess distribution fit.

The contour plot (Figure 18) indicates two predictor variables and shows the association between the variables which are days, burners, and engines that are used for the treatments. The dark areas of the plot specify excellence.

3.4.5. The 3D Scatterplot Plot of Response vs. Day vs. Engine Surface Plot of Day vs. Engine vs. Burner. The graph of three dimensional (3D) graph (Figure 19) and surface plot (Figure 20) of illustration into two predictor variables and related the response variable is represented above the maximum quality scores and occur at about the second engine of the third day of the second burner treatment is 12.

All the sum of squares is presented in the ANOVA Table 8 and inference is given below.

(1) Inference. Since the p values are 0.043, 0.5, and 0.048, there is a difference between the burners and the days, but the difference between engines is not significant.

4. Conclusion

(i) This study proposed an optimization method of construction for warping copper plates and engines using complete block designs with bipartite and complete bipartite graphs.

(ii) The first method of construction for RBD with the numerical example is to test whether there is any significant difference between labs and warping copper plates with specimens discussed, construing the graphs of results is an interaction plot for response lines around parallel, so our hypothesis of the study is valid and significant.

(iii) Therefore, inference of P is 0.001 and the model F-value (63.02) suggests that the model is significant and only a 0.001% chance that an F-value this large could occur due to noise.

(iv) Also, the calculated R^2 value is nearest to 1 (0.9666) and the model is fitted to our problem, and the R^2 probability value is 0 to 1 and the difference is very close, i.e, R^2 to adjusted R^2 (0.9072) and the noise signal is greater than four (27) and also the predicted R^2 value is 90.72% which is substantially less than R^2 value of 96.66% which may indicate overall warping copper plates and engines are fitted.

(v) Finally, it was concluded that the relationship between the variables of labs and treatments for the amount of warping (mm) of copper plates occurs at nearly the second lab = 590 and warping copper plates and specimens D is efficient with the 3D surface.

(vi) The second optimization method of construction for burners and engines using LSD with a regular graph is to test whether there is any significant difference between burners, days, and engines.

(vii) The interaction graphs of the lines are not parallel, and the inference is that the P values are 0.043, 0.5, and 0.048 (less than 0.05, reject the hypothesis). Hence, the conclusion is that the burners and the days are different. The difference between engines is insignificant, but the model fits because the R_2 value is nearest to 1 (0.9774, and the probability R_2 value is 0 to 1).

(viii) The difference is very close R^2 to the adjusted R^2 (0.9072) and the noise signal is greater than 4 (88) and also the predicted R^2 value is 54.27% which is substantially less than the R^2 value of 97.74% which may indicate that the overall model is fitted.

(ix) The 3D scatterplot and the 3D surface plot show the three predictor variables (days, burners, and engines). In our study, the maximum quality score at about the second engine on the third day of the second burner treatment is 12.

(x) This methodology can also be applied in the case of factorial experiments, confounding, fractional replicated designs, balanced incomplete block designs, lattice designs, and so on.

Data Availability

The data that support the findings of this study are available from the corresponding author on request.

Conflicts of Interest

The authors declare that they have no conflicts of interest.

References

[1] J. A. Bondy and U. S. R. Murty, *Graph Theory with Applications"*, Elsevier Science Publishing Co Inc, New York, NY, USA, 1976.

[2] M. N. Das and N. C Giri, *Design and Analysis of Experiment"*, New Age International (P) Limited, New Delhi, India, 1979.

[3] R. C. Bose, *On the Construction of Balanced Incomplete Block Designs", Human Genetics*, UCL and Blackwell Publishing Ltd, Hoboken, NJ, USA, 1939.

[4] S. Yamamoto, H. Ikeda, S. Shige-Eda, K. Ushio, and N. Hamada, "On claw decomposition of complete graphs and complete bipartite graphs," *Hiroshima Mathematical Journal*, vol. 5, no. 1, pp. 33–42, 1975.

[5] C.-Q. Zhang and Y.-J. Zhu, "Factorizations of regular graphs," *Journal of Combinatorial Theory - Series B*, vol. 56, no. 1, pp. 74–89, 1992.

[6] W. Zhang, D. S. Wu, Y. Lee, and B. Masterson, “The effect of underfill epoxy on warpage in flip-chip assemblies,” *IEEE Transactions on Components Packaging and Manufacturing Technology Part A*, vol. 21, no. 2, pp. 323–329, 1998.

[7] D. J. Jacobs, A. Rader, L. A. Kuhn, and M. Thorpe, “Protein flexibility predictions using graph theory,” *Proteins: Structure, Function, and Genetics*, vol. 44, no. 2, pp. 150–165, 2001.

[8] A. L. Gavrilyuk and A. A. Makhnev, “Amply regular graphs and block designs,” *Siberian Mathematical Journal*, vol. 47, no. 4, pp. 621–633, 2006.

[9] H. C. Tseng, C. Hung, and C. C. Huang, “An analysis of the formability of aluminum/copper clad metals with different thicknesses by the finite element method and experiment,” *International Journal of Advanced Manufacturing Technology*, vol. 49, no. 12, pp. 1029–1036, 2010.

[10] V. Z. Rizzo and R. D. Mansano, “Electro-optically sensitive diamond-like carbon thin films deposited by reactive magnetron sputtering for electronic device applications,” *Progress in Organic Coatings*, vol. 70, no. 4, pp. 365–368, 2011.

[11] S. Miyajima, S. Nagamatsu, S. S. Pandey, S. Hayase, K. Kaneto, and W. Takashima, “Electrophoretic deposition onto an insulator for thin film preparation toward electronic device fabrication,” *Applied Physics Letters*, vol. 101, no. 19, Article ID 193305, 2012.

[12] S. Y. Yang, W. S. Kwon, and S. B. Lee, “Chip warpage model for reliability prediction of delamination failures,” *Microelectronics Reliability*, vol. 52, no. 4, pp. 718–724, 2012.

[13] M. Pachamuthu and R. Jaisankar, “Construction of lattice designs using MOLS,” *Malaya Journal of Matematik*, no. 1, pp. 11–16, 2013.

[14] A. Gupta, L. Barron, M. Brainin, and J. B. Lee, “Reduction of out-of-plane Warpage in surface Micromachined beams using corrugation,” *Journal of Micromechanics and Microengineering*, vol. 24, no. 6, Article ID 065023, 2014.

[15] W. T. Federer and J. Wright, *Construction of Lattice Square Designs”*, Technical Report Series of the Biometrics Unit, Cornell University, Ithaca, NY, USA, 1986.

[16] Y. M. Hwang and G. Y. Tzou, “An analytical approach to asymmetrical cold- and hot-rolling of clad sheet using the slab method,” *Journal Of Materials Processing Technology*, vol. 62, no. 1–3, pp. 249–259, 1996.

[17] C. H. Lee, J. P. Park, and Y. H. Moon, “Differential speed rolling to reduce warping in bimetallic slab,” *Advances in Mechanical Engineering*, vol. 6, pp. 375162–375167, 2014.

[18] C. Zhu, W. Ning, H. Lee, J. Ye, G. Xu, and L. Luo, “Experimental identification of warpage origination during the wafer level packaging process,” in *Proceedings of the IEEE 64th Electronic Components And Technology Conference (ECTC)*, pp. 815–820, IEEE, Lake Buena Vista, Florida, USA, May 2014.

[19] C. Kim, T. I. Lee, M. Kim, and T. S. Kim, “Warpage analysis of electroplated Cu films on fiber- reinforced polymer packaging substrates,” *Polymers*, vol. 7, no. 6, pp. 985–1004, 2015.

[20] H. C. Lee, “Decomposition of the complete bipartite multigraph into cycles and stars,” *Discrete Mathematics*, vol. 338, no. 8, pp. 1362–1369, 2015.

[21] B. N. Mandal and S. Dash, “On balanced incomplete Latin square designs,” *Communications in Statistics - Theory and Methods*, vol. 46, no. 13, pp. 6258–6263, 2017.

[22] M. N. F. Sumaiya, W. V. Nishadi, K. D. E. Dhananjaya, A. A. I. Perera, and D. Uththamawadu, “Generation of compete bipartite graphs using normalized hadamard matrices,” *Elixir Appl. Math.*vol. 113, pp. 49269–49271, 2017.

[23] A. Ramya and M. Pachamuthu, “On the construction of balanced incomplete block designs through factorization and coloring graphs using mutually orthogonal Latin square designs,” *International Journal of Agricultural Statistics Science*, vol. 15, no. 2, pp. 807–813, 2019.

[24] M. Ilayaraja and A. Muthusamy, “Decomposition of complete bipartite graphs into cycles and stars with four edges,” *AKCE International Journal of Graphs and Combinatorics*, vol. 17, no. 3, pp. 697–702, 2020.

[25] V. Sivamaran, B. Visvalingam, G. Mannathusamy, and V. Viswanathan, A. G. Rao, Effect of chemical vapor deposition parameters on the diameter of multi-walled carbon nanotubes,” *International Nano Letters*, Springer, vol. 8, no. 4, pp. 1–12, 2018.

[26] V. Sivamaran, V. Balasubramanian, M. Gopalakrishnan, V. Viswabaskaran, and A. Gouravrao, “Optimizing chemical vapor deposition parameters to attain minimum diameter carbon nano tubes by response surface methodology,” *Journal of Advanced Microscopy Research*, vol. 13, no. 2, pp. 181–189, 2018.

[27] M. A. Nemitallah, A. A. Abdelhafez, A. Ali, I. Mansir, and M. A. Habib, “Frontiers in combustion techniques and burner designs for emissions control and CO2 capture- A Review,” *International Journal Of Energy Research*, pp. er.4730–33, 2019.

[28] V. Sivamaran, V. Balasubramanian, M. Gopalakrishnan, V. Viswabaskaran, and A. G. Rao, “Identification of appropriate catalyst system for the growth of multi-walled carbon nanotubes via catalytic chemical vapor deposition process in A single step batch technique,” *Materials Research Express*, vol. 6, no. 10, pp. 105620–105716, 2019.

[29] P. S. K. Reddy and P. S. Hemavathi, “Generalization of bipartite graphs,” *Journal of Discrete Mathematical Sciences and Cryptography*, vol. 23, no. 3, pp. 787–793, 2020.

[30] S. Saurabh and M. K. Singh, “A note on the construction of Latin square type designs,” *Communications in Statistics - Theory and Methods*, vol. 51, no. 10, pp. 3434–3437, 2020.

[31] I. Ozkan, “Investigation on the electromagnetic shielding performance of copper plate and copper composite fabrics: a comparative study,” *Tekstil ve Konfeksiyon*, vol. 30, no. 2, pp. 156–162, 2020.

[32] I. Raza and M. Asif Masood, “Efficiency of lattice design in relation to randomized complete block design in agricultural field experiments,” *Pakistan Journal Of Agricultural Research*, vol. 22, no. 3-4, pp. 150–153, 2009.

[33] T. Richthammer, “Bunkbed conjecture for complete bipartite graphs and related classes of graphs,” 2022, https://arxiv.org/abs/2204.12931.

[34] G. Braun and H. Tyagi, “Minimax optimal clustering of bipartite graphs with a generalized power method,” 2022, https://arxiv.org/abs/2205.12104.

[35] V. Sivamaran, V. Kavimani, M. Bakkiyaraj, and S. T. Selvamani, “Multi response optimization on tribo-mechanical properties of CNTs/nSiC reinforced hybrid Al MMC through RSM approach,” *Forces in Mechanics*, Elsevier, vol. 6, pp. 1–17, Article ID 100069, 2022.